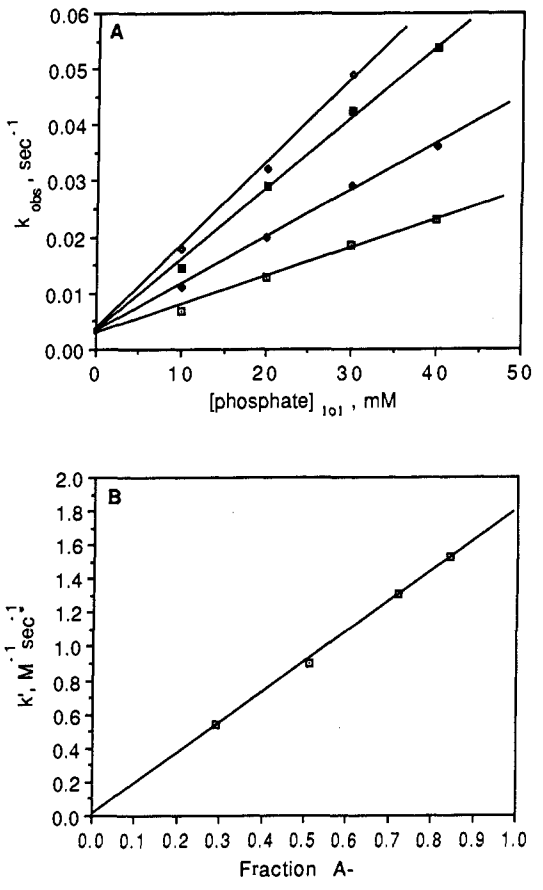

Figure 1. (A) Plot of the observed first-order rate constants vs total buffer concentration for the ketonization of enolpyruvate at various fixed pD levels at 20 °C. Reactions were run in the presence of 10–40 mM phosphate buffer at the following fixed pD levels: 7.0 (□), 7.4 (◇), 7.8 (■), and 8.1 (◆). Ionic strength was maintained at 0.1 by the addition of KCl. (B) The dependence of k' ($k_{obsd}-k_0$/[phosphate]) on the mole fraction of the general base DPO_3^{2-}.

served by Rose et al., ketonization is severalfold faster in H_2O than in D_2O.[10] This same method of generating enols in aqueous buffer solutions has previously been used to study ketonization of monofunctional enols.[11]

When TMS-enolpyruvate was dissolved in d_3-acetonitrile, the NMR spectrum showed doublets for two nonequivalent vinyl protons at 5.50 and 4.93 ppm (J = 0.87 Hz), along with TMS peaks at 0.2 and 0.3 ppm. Low-intensity doublets at 4.83 and 5.10 ppm, presumably from a small amount of TMS-enolpyruvic acid, were also observed. Upon addition of a small amount of D_2O, the two vinyl signals were rapidly replaced by doublets at 4.77 and 5.06 ppm (J = 1.26 Hz). These signals then decayed over several minutes with concomitant increase of a triplet at 2.35 ppm corresponding to monodeuterated pyruvate. This suggests that both the TMS ester and TMS ether cleavage reactions are fast and the ketonization step is rate-determining. Similar results were observed in pure D_2O solvent.

The rates of the ketonization of enolpyruvate were studied in phosphate buffers in D_2O over a pD range of 7.0–8.1 (Figure 1). Least-squares analysis of these data gave a good fit with a pH-independent intercept rate constant of 2.0 ± 0.1 × 10^{-3} s^{-1} and a zero intercept in the replot at zero $H_2PO_4^-$ concentration, indicating that only general base catalysis or the kinetically indistinguishable specific base–general acid catalysis operates.[12] The apparent general base rate constant is 1.81 ± 0.05 M^{-1} s^{-1} at 20 °C. Analysis of the data by the method of Kresge[8,13] reveals that the reaction proceeds entirely through the enolate and thus follows the specific base–general acid mechanism. If the pK_a of enolpyruvate is assumed[6] to be 12, the bimolecular rate constant for protonation of the enolate by $H_2PO_4^-$ ion is 8 × 10^4 M^{-1} s^{-1}.

Enolpyruvate is generated efficiently and quickly by the method described here. The enol undergoes buffer-catalyzed ketonization to give pyruvate in a manner consistent with that of a variety of other enols. The data presented here suggest that enolpyruvate is sufficiently stable in solutions of low buffer content ($t_{1/2}$ = 1.8 min in 10 mM phosphate buffer, pD 7.0, 20 °C or 7 min at zero buffer concentration) to allow studies of its intermediary role in enzyme-catalyzed reactions.

(10) The rate difference between reactions in H_2O and in D_2O depends on the assumption made about effects of D_2O on buffer pK_a values. Our experience suggests that, at the same concentration of buffer, the solvent isotope effect is about 3.

(11) Chiang, Y.; Kresge, A. J.; Walsh, P. A. *J. Am. Chem. Soc.* **1986**, *108*, 6314.

(12) Jencks, W. P. *Catalysis in Chemistry and Enzymology*; McGraw-Hill: New York, 1969; pp 163–242.

(13) Kresge, A. J. *Chem.-Tech. (Heidelberg)* **1986**, *16*, 250.

Multiphasic Intracomplex Electron Transfer from Cytochrome *c* to Zn Cytochrome *c* Peroxidase: Conformational Control of Reactivity

Sten A. Wallin,[1a] Eric D. A. Stemp,[1a] Andrew M. Everest,[1a] Judith M. Nocek,[1a] Thomas L. Netzel,*[1b,c] and Brian M. Hoffman*[1a]

Department of Chemistry, Northwestern University Evanston, Illinois 60208
Amoco Technology Company, Naperville, Illinois 60566
Received June 14, 1990

We have shown recently that the photoinitiated ^{3}(MP) → Fe^{3+}P (P = porphyrin; M = Zn, Mg) and subsequent thermal Fe^{2+}P → (MP)$^+$ electron transfer (ET) process within mixed-metal hemoglobin hybrids can be described by a kinetic mechanism suitable for a conformationally rigid system, Scheme I.[2] Our early data for the same ET processes within [ZnCcP,Cc] complexes (ZnCcP = zinc-substituted cytochrome *c* peroxidase, Cc = cytochrome *c*) also was interpreted with Scheme I.[3] However, data obtained with improved signal/noise now shows that the I → A process in [ZnCcP,Cc] cannot be described by this simple scheme and indicates that the electron-transfer intermediate, [(ZnP)$^+$CcP,Fe^{2+}P] (I), exists in multiple bound forms that exhibit remarkably different rate constants for the Fe^{2+}P → (ZnP)$^+$ ET reaction.

The triplet state, A*, of the [ZnCcP,Fe^{3+}Cc] complex decays exponentially when excess Fe^{3+}Cc is present.[4] Scheme I for a rigid complex then predicts that I appears with the larger of the triplet decay and thermal ET rate constants, k_p and k_b, respectively, and disappears with the smaller according to the equation

$$[I(t)] = [A^*(0)]k_t\frac{\{e^{-k_p t} - e^{k_b t}\}}{k_b - k_p} \quad (1)$$

In our original examination of [ZnCcP,Cc] complexes, we detected a slowly decaying kinetic transient for I when using a vertebrate Cc (tuna), $k_b \sim 30\ s^{-1} < k_p$, but a rapidly appearing transient with a fungal Cc (yeast iso-1), $k_b \sim 10^4\ s^{-1} > k_p$.[3] High-sensitivity

(1) (a) Northwestern University. (b) Amoco Technology Company. (c) Present Address: Department of Chemistry, Georgia State University, Atlanta, GA 30303.

(2) (a) Natan, M. J.; Hoffman, B. M. *J. Am. Chem. Soc.* **1989**, *111*, 6468–6470. (b) Natan, M. J.; Kuila, D.; Baxter, W. W.; King, B. C.; Hawkridge, F. M.; Hoffman, B. M. *J. Am. Chem. Soc.* **1990**, *112*, 4081–4082.

(3) (a) Ho, P. S.; Sutoris, C.; Liang, N.; Margoliash, E.; Hoffman, B. M. *J. Am. Chem. Soc.* **1985**, *107*, 1070–1071. (b) Liang, N.; Kang, C. H.; Ho, P. S.; Margoliash, E.; Hoffman, B. M. *J. Am. Chem. Soc.* **1986**, *108*, 4665–4666. (c) Liang, N.; Pielak, G. J.; Mauk, A. G.; Smith, M.; Hoffman, B. M. *Proc. Natl. Acad. Sci. U.S.A.* **1987**, *84*, 1249–1252. (d) Liang, N.; Mauk, A. G.; Pielak, G. J.; Johnson, J. A.; Smith, M.; Hoffman, B. M. *Science (Washington, D.C)* **1988**, *240*, 311–313. (e) Liang, N. Ph.D. Dissertation, Northwestern University, 1988.

(4) The decay of A* was followed both by ^{3}ZnP emission and by ^{3}ZnP transient absorption at λ = 475 nm. Differences in k_p for the two Cc represent differences in both the rate constants for quenching by the ferriheme and in affinity constants.

0002-7863/91/1513-1842$02.50/0

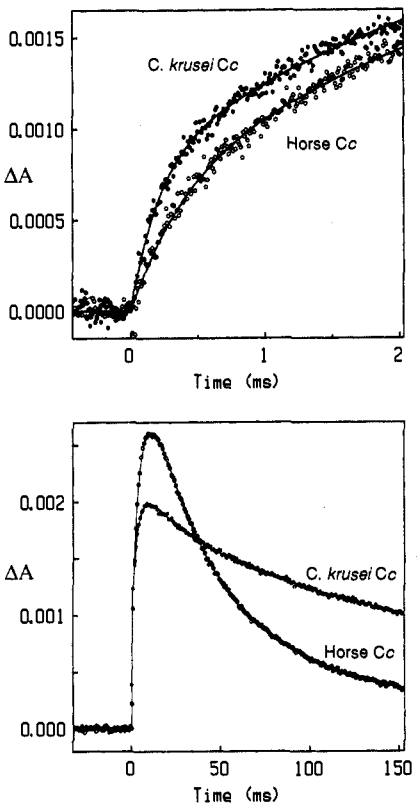

Figure 1. Kinetic progress curves (λ = 549 nm, 20 °C) for electron-transfer intermediate, I, formed upon flash photolysis of [ZnC*c*P,C*c*] complexes: (○) horse C*c* (4.7 μM ZnC*c*P, 14.2 μM C*c* in 5 mM KP_i, pH 7); (●) *C. krusei* C*c* (5.5 μM ZnC*c*P, 12.1 μM C*c* in 1 mM KP_i, pH 7). Solid lines are fits as described in footnote 7. The parameters used for the horse and *C. krusei* C*c* traces, respectively are: k_p = 150, 296 s^{-1}; k_1 = 2420, 3760 s^{-1}; k_2 = 38.1, 40.1 s^{-1}; k_3 = 8.8, 3.7 s^{-1}; f_1 = 0.76, 0.82; f_2 = 0.19, 0.04; f_3 = 0.05, 0.14.

Scheme I

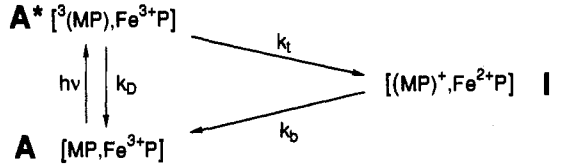

transient absorption measurements now show that the temporal evolution of I *cannot* be described by the simple cycle of Scheme I: for complexes with both the vertebrate and fungal C*c*, the transient-absorbance change due to I not only rises in a biphasic fashion where one of the rate constants is greater than k_p (Figure 1, upper) but also falls in a multiphasic fashion with components that decay more slowly than k_p (Figure 1, lower).[5]

Excellent self-consistent fits to data collected over both short and long times (Figure 1) can be obtained by summing three kinetic phases of the form of eq 1, each constrained to have k_p equal to the observed triplet decay, but each with its own value of k_b (k_i, i = 1–3).[6,7] These fits reveal that for both C*c* the majority of the I → A reaction (phase 1, $f_1 \sim 0.8$) occurs with a k_b rate constant much larger than k_p: k_1 = 2500 (500) and 3500 (500) s^{-1} for horse and *Candida krusei* C*c* complexes, respectively. In both cases the remainder (phases 2 and 3) occurs ca. 2–3 orders of magnitude more slowly, with $k_b < k_p$ (Figure 1). The kinetic spectra of phases 2 and 3 have been examined after the decay of A* ($t \geq 10/k_p$) and individually match the spectrum predicted[3d,e] for I. The rapidly appearing component, phase 1, can be detected without spectral interference from A* only *near* an A*/A isosbestic because it decays synchronously with A*. However, it too can be assigned to I because identical fits to the multiphasic kinetics are observed at the 549-nm isosbestic (Figure 1) where only the FeP redox change is monitored, and at the 445-nm isosbestic where the ZnP and FeP redox changes are detected with comparable weight.[3d,e] In short, all three kinetic phases are associated with the ET intermediate, I. The fits indicate that the manifest difference between the long-time decays for the two complexes (Figure 1, lower) in fact primarily reflects differences in the amounts of the two minority phases.[6] Preliminary observations[9] show that the same is true for yeast iso-1 C*c* and tuna C*c* studied earlier.[3b,d]

Scheme II

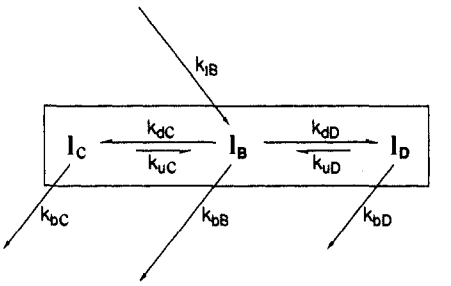

The slow component of the I → A process does not reflect the second-order recombination of free (ZnP+)C*c*P and Fe^{2+}C*c* formed by dissociation of I because the long-time decay cannot be fit by a second-order equation and the rate constants for these phases do not change appreciably upon variation of either (i) the concentration of I produced by varying the actinic flash intensity or (ii) the amount of excess Fe^{3+}C*c* in the sample solution.[9,10] Chemically distinct forms of the complex do not appear to be responsible for the multiphasic kinetics because (i) both ZnC*c*P and the cytochromes are homogeneous as judged by HPLC and IEF and (ii) the relative fractions of the different phases change with C*c* and solution conditions. Rather we interpret the observed kinetics to imply that state I exists in multiple bound forms with widely different ET reactivities.

A variety of considerations[8,11-14] suggest that these bound forms

(5) (a) Deoxygenated samples contained 3–6 μM ZnC*c*P, with [C*c*]/[ZnC*c*P] typically ~2/1 in pH 7 KP_i buffers (μ = 0.0015–0.015). The binding constants for the two C*c* are not the same; for a given C*c* the ratio was normally held constant so that, if a second binding site for C*c* is involved,[5b] occupancies would be fixed. The transient absorption apparatus employs a frequency-doubled Nd:YAG laser as the excitation source (6-ns pulse width, λ = 532 nm), home-built detection electronics with a bandwidth of ~1 MHz, and an EPIC Instruments 10v3 transient digitizer (4K, 8 bit points) interfaced to a PC clone.[5c] Typically 250–500 transients were averaged for short-time traces (in contrast to earlier measurements which were instrumentally limited to ≤30 transients), 50–100 for long-time. The absence of any transients faster than those reported here was ascertained from measurements obtained with an instrument with a shorter response time (200-MHz bandwidth, 25-ps excitation at 532 nm).[5d-f] (b) Kornblatt, J. A.; English, A. M. *Eur. J. Biochem.* **1986**, *155*, 505–511. (c) Wallin, S. A.; Hoffman, B. M., to be published. (d) Winkler, J. R.; Netzel, T. L.; Creutz, C.; Sutin, N. *J. Am. Chem. Soc.* **1987**, *109*, 2381. (e) Winkler, J. R.; Nocera, D. G.; Netzel, T. L. *J. Am. Chem. Soc.* **1986**, *108*, 4451. (f) Stinson, S. *Chem. Eng. News* **1986**, *21* (July 28).

(6) Data traces for $I(t)$ were fit to the function $\Delta A(t) = \{\beta\sum f_i(\exp(-k_p t) - \exp(-k_i t))/(k_i - k_p)\} + A_{trp}\exp(-k_p t)$, where i = 1, 2, 3; $\beta = k_r\Delta\epsilon_I[A^*(0)]$; k_i is the I → A rate for phase i; f_i is the number average weight of each kinetic phase; and A_{trp} corrects for departures from the A*/A isosbestic.

(7) As discussed in ref 8 and references therein, direct differentiation between a description in terms of two slowly decaying phases (2 and 3) and a distribution of slowly decaying phases is not possible; we have chosen the former for simplicity and clarity.

(8) Nocek, J. M.; Liang, N.; Wallin, S. A.; Mauk, A. G.; Hoffman, B. M. *J. Am. Chem. Soc.* **1990**, *112*, 1623–1625.

(9) To be published.

(10) However, the small amplitude and slow decay of phase 3 does make it difficult to prove that this phase is totally uncontaminated by second-order processes.

(11) Poulos, T. L.; Sheriff, S.; Howard, A. J. *J. Biol. Chem.* **1987**, *272*, 13881–13883.

(12) (a) Satterlee, J. D.; Moench, S. J.; Erman, J. E. *Biochim. Biophys. Acta* **1987**, *912*, 87–97. (b) Englander, W. Presented at the 199th National Meeting of the American Chemical Society, Boston, MA, April 26, 1990; Abstract BIOL 135. (c) McLendon, G. Presented at the 199th National Meeting of the American Chemical Society, Boston, MA, April 26, 1990; Abstract BIOL 138.

may represent *dynamically* interconverting conformational substates. The simplest mechanism that incorporates this suggestion and satisfactorily describes the present data includes three such substates (Scheme II). In this mechanism, the ^{3}(ZnP) → Fe^{3+}P ET reaction occurs only within one form, B, of A* to produce the corresponding form of I. This substate, I_B, undergoes rapid ET to regenerate A, but it is not the most stable form of I and concurrently rearranges to two substates, I_C and I_D,[15] that are more stable but much less reactive. Experiments are now in progress to test this and other models, to examine whether the suggested conformational changes are interfacial or intraprotein,[13d] and to explain the sharply different values of k_b among the conformational substates of the complex.

Acknowledgment. We thank R. J. Loyd and W. Humer for their assistance and our collaborators, Professors E. Margoliash, A. G. Mauk, and M. A. Ratner. This work has been supported by the NIH (HL 13531) and NSF (DMB 8907559).

(13) (a) Hoffman, B. M.; Ratner, M. A.; Wallin, S. A. In *Electron Transfer in Biology and the Solid State: Inorganic Compounds with Unusual Properties*; Johnson, M. K., et al., Eds.; Advances in Chemistry 226; American Chemical Society: Washington, DC, 1990; pp 125-146. (b) Hoffman, B. M.; Ratner, M. A. *J. Am. Chem. Soc.* **1987**, *109*, 6237-6243. Erratum: *J. Am. Chem. Soc.* **1988**, *110*, 8267. (c) McLendon, G.; Pardue, K.; Bak, P. *J. Am. Chem. Soc.* **1987**, *109*, 7540-7542. (d) Yuan, X.; Songcheng, S.; Hawkridge, F. M. *J. Am. Chem. Soc.* **1990**, *112*, 5380-5381.

(14) (a) Hazzard, J. T.; McLendon, G.; Cusanovich, M. A.; Das, G.; Sherman, F.; Tollin, G. *Biochemistry* **1988**, *27*, 4445-4451. (b) Kang, C. H.; Ferguson-Miller, S.; Margoliash, E. *J. Biol. Chem.* **1977**, *252*, 919-926.

(15) The microscopic rate constants for Scheme II are obtained from the fits to the kinetic progress curves (Figure 1 and footnote 7) as follows; $k_{bB} \sim f_1k_1$; $k_{dC} \sim f_2k_1$; $k_{dD} \sim f_3k_1$; $k_2 \sim k_{bC} + k_{uC}$; $k_3 \sim k_{bD} + k_{uD}$. Setting $k_{uC} \sim k_{uD} \sim 0$ gives the lowest value for the ratio of ET rate constants: $k_{bB}/k_{bC} \approx k_1/k_2$ and $k_{bB}/k_{bD} \approx k_1/k_3$.

A Very Large Calcium Dialkoxide Molecular Aggregate Having a CdI_2 Core Geometry: $Ca_9(OCH_2CH_2OMe)_{18}(HOCH_2CH_2OMe)_2$

Subhash C. Goel, Michael A. Matchett, Michael Y. Chiang, and William E. Buhro*

Department of Chemistry, Washington University
St. Louis, Missouri 63130
Received October 12, 1990

Herein we describe the first molecular calcium dialkoxide.[1] The aggregate size exhibited by the title compound is among the *largest* known for alkoxide complexes,[2] yet demonstrates Bradley's classic structural theory[3] which states (in part) that metal alkoxides will adopt the *smallest* degree of aggregation that permits the metal atoms to attain their preferred coordination numbers. The structure of $Ca_9(OCH_2CH_2OMe)_{18}(HOCH_2CH_2OMe)_2$ (**1**) helps to rationalize the general properties of group 2 alkoxides.

Compound **1** was prepared by interaction of calcium filings and 2-methoxyethanol (ratio 1.0 g atom to 2.5 mol, respectively) in refluxing hexane and was crystallized from the filtered reaction mixture as small needles (64% yield).[4] The molecular structure[5] of **1** (Figures 1 and 2) contains three 6-coordinate and six 7-coordinate calcium atoms for an average coordination number (CN_{av}) of 6.67. The central $Ca_9(\mu_3\text{-}O)_8(\mu_2\text{-}O)_8O_{20}$ core (Figure 2) mimics the layer structure of CdI_2 (except at the periphery) in that nine coplanar calcium atoms occupy octahedral holes between two close-packed oxygen layers. Significantly, the

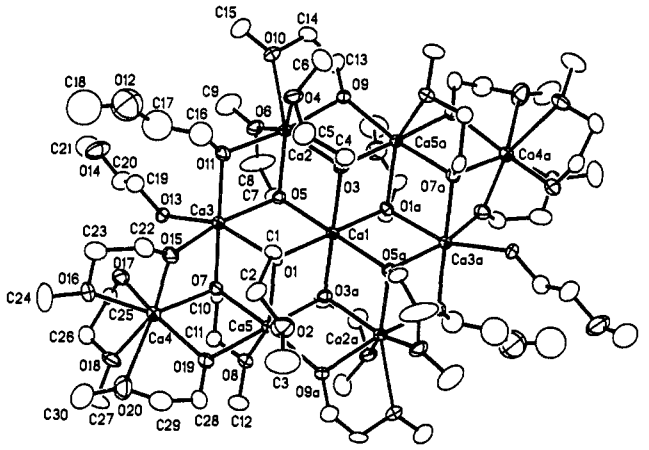

Figure 1. ORTEP of $Ca_9(OCH_2CH_2OMe)_{18}(HOCH_2CH_2OMe)_2$ (**1**). Average distances (Å): Ca-(μ_3-O), 2.390 (8); Ca-(μ_2-O), 2.291 (8); Ca-O_{ether}, 2.60 (1). Other distances (Å): Ca(3)-O(13), 2.455 (7); Ca(4)-O(17), 2.313 (9). The longer Ca(3)-O(13) separation likely pertains to the 2-methoxyethanol ligand.

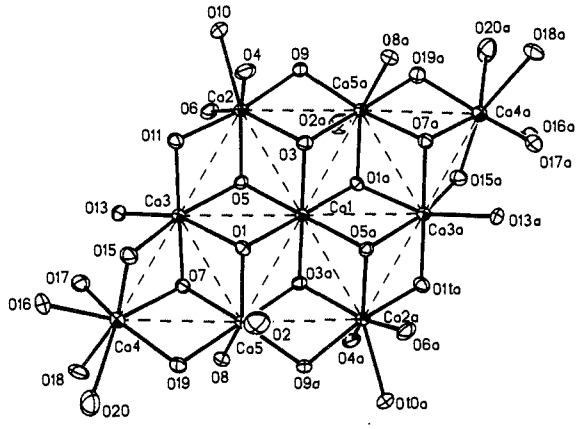

Figure 2. View of the central $Ca_9(\mu_3\text{-}O)_8(\mu_2\text{-}O)_8O_{20}$ core of **1**.

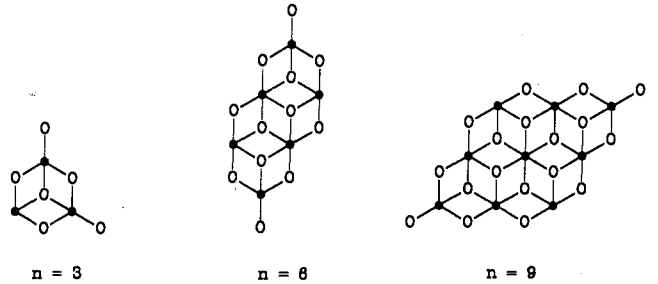

Figure 3. Sample calculations using a CdI_2-based model for [Ca-$(OCH_2CH_2OMe)_2]_n$ oligomers having n = 3, 6, and 9. The small, filled circles represent calcium atoms and the larger, open circles represent alkoxide oxygen atoms of the 2-methoxyethoxide ligands. Note that each *ligand* also participates in one Ca-O_{ether} dative bond (not shown).

(1) Calcium *aryl*oxide complexes have been reported.[1a-c] Several recent studies claim to employ soluble calcium alkoxides; however, these substances are uncharacterized.[1d-f] (a) Hitchcock, P. B.; Lappert, M. F.; Lawless, G. A.; Royo, B. *J. Chem. Soc., Chem. Commun.* **1990**, 1141. (b) McCormick, M. J.; Moon, K. B.; Jones, S. R.; Hanusa, T. P. *J. Chem. Soc., Chem. Commun.* **1990**, 778. (c) Cole, L. B.; Holt, E. M. *J. Chem. Soc., Perkin Trans. 2* **1986**, 1997. (d) Hirano, S.; Hayashi, T.; Tomonaga, H. *Jpn. J. Appl. Phys.* **1990**, *29*, L40. (e) Nonaka, T.; Green, M.; Kishio, K.; Hasegawa, T.; Kitazawa, K.; Kaneko, K.; Kobayashi, K. *Physica C* **1989**, *160*, 517. (f) Kobayashi, T.; Nomura, K.; Uchikawa, F.; Masumi, T.; Uehara, Y. *Jpn. J. Appl. Phys.* **1988**, *27*, L1880.

(2) To our knowledge the largest structurally characterized molecular alkoxide aggregate is the cyclic decamer $[Y(OCH_2CH_2OMe)_3]_{10}$: Poncelet, O.; Hubert-Pfalzgraf, L. G.; Daran, J.-C.; Astier, R. *J. Chem. Soc., Chem. Commun.* **1989**, 1846.

(3) Bradley, D. C. *Nature* **1958**, *182*, 1211.

(4) Satisfactory elemental (C, H, Ca) and spectroscopic analyses were obtained. See the supplementary material.

(5) Crystal data for **1**: $C_{60}H_{142}Ca_9O_{40}$, M_r = 1864.5, triclinic, $P\bar{1}$, a = 10.220 (4) Å, b = 15.515 (5) Å, c = 15.991 (4) Å, α = 67.29 (2)°, β = 87.17 (3)°, γ = 80.98 (3)°, V = 2309.9 (13) Å^3, T = 295 K, Z = 1, D_{calcd} = 1.340 g cm^{-3}, λ(Mo Kα) = 0.71073 Å. Of the 8176 unique intensities measured, 3123 with $F_o > 6.0\sigma(F_o)$ yielded $R(F)$ = 0.0666 and $R_w(F)$ = 0.0354.

0002-7863/91/1513-1844$02.50/0